DOI: 10.1002/ejic.201100264

New Pyridazine-Bridged NHC/Pyrazole Ligands and Their Sequential Silver(I) Coordination

Jan Wimberg,[a] Ulrich J. Scheele,[a] Sebastian Dechert,[a] and Franc Meyer*[a]

Keywords: Carbene ligands / Nitrogen heterocycles / Ligand design / Silver / Oligometallic complexes

A family of new pyridazine-bridged NHC/pyrazole ligand precursors $HL^{1–5}$ were prepared and fully characterized including analysis by XRD {HL^1 = 3-[3-(2,6-diisopropylphenyl)-3*H*-imidazolium-1-yl]-6-(3-pyridin-2-yl-pyrazol-1-yl)-pyridazine, HL^2 = 3-[3-(2,4,6-trimethylphenyl)-3*H*-imidazolium-1-yl]-6-(3-pyridin-2-yl-pyrazol-1-yl)-pyridazine, HL^3 = 3-[3-(2,4,6-trimethylphenyl)-3*H*-imidazolium-1-yl]-6-(3,5-dimethylpyrazol-1-yl)-pyridazine, HL^4 = 3-(3-*tert*-butyl-3*H*-imidazolium-1-yl)-6-(3,5-dimethylpyrazol-1-yl)-pyridazine, HL^5 = 3-[3-(2,4,6-trimethylphenyl)-3*H*-imidazolium-1-yl]-6-(3-methyl-5-phenylpyrazol-1-yl)-pyridazine, X = PF_6^- or BF_4^-}. Reaction of the ligand precursors with Ag_2O yielded various silver(I) complexes whose structures have been elucidated crystallographically. In complexes $[(L^3)_2Ag](PF_6)$ (**4**) and $[(L^4)_2Ag](PF_6)$ (**4′**) the single silver(I) ion is coordinated in a linear fashion by the NHC moieties of the two ligand strands. An NMR titration with $AgBF_4$ reveals that **4** can bind two more silver(I) ions. The complex $[(L^5)_2Ag_2](PF_6)_2$ (**5′**) features an additional silver(I) centre bound to the two pyrazole rings, whereas in $[(L^3)_2Ag_2](BF_4)_2$ (**6**) ligand reshuffling has occurred to give antiparallel ligand strands with $\{C^{NHC}N^{pyrazole}\}$ coordination of each metal ion. Secondary interactions with the pyridazine N-atom are observed in some cases. An additional third silver(I) ion can be accommodated between the central pyridazine bridges, as shown in $[(L^3)_2Ag_3](PF_6)_2(BF_4)$ (**7**). The sequence of binding events and the identity of the species in solution have been investigated by NMR spectroscopy and ESI mass spectrometry.

Introduction

N-Heterocyclic carbenes (NHCs) are currently among the most popular ligands in transition-metal chemistry and are finding widespread use in catalysis.[1,2] As part of their further elaboration, NHC units in recent years have been increasingly incorporated in multidentate ligand scaffolds,[3] including compartmental ligands for di- and oligometallic complexes.[4,5] Such complexes in which two (or more) metal ions are held in close proximity offer interesting perspectives for catalytic applications, as new reaction pathways may become available if the adjacent metal centres act in concert.[6] Although the number of symmetric dinucleating ligands with two identical binding pockets is growing rapidly,[7] asymmetric dinucleating ligands that feature two different compartments are still relatively scarce.[8] Interest in such asymmetric systems stems from the expectation that they may enable the targeted synthesis of preorganized heterodimetallic complexes in which the metal centres play distinct roles during cooperative action.[6a,9]

Pyridazine is well established as a versatile bridging unit that is capable of spanning two metal ions through its two N-atoms, with metal–metal distances suitable for cooperativity.[10] Starting from cheap 3,6-dichloropyridazine, chelate arms may be readily attached to the 3- and 6-positions of the pyridazine bridge in order to increase preorganization of the dimetallic array.[11] The simple pyridazine/NHC hybrid ligands **A** (Scheme 1) have previously been employed in palladium chemistry,[12] and the dinucleating type **B** scaffolds have been used for the synthesis of oligonuclear mercury(II) and silver(I) complexes.[13]

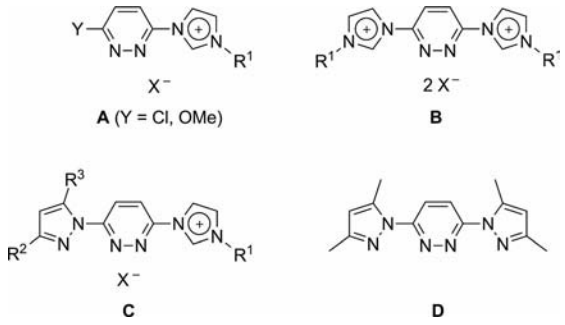

Scheme 1.

Silver(I) complexes of NHC-based ligands are attracting much attention because of their large structural diversity,[14] their potentially interesting photophysical properties[15] and their convenient use in transmetallation reactions for the preparation of various other NHC complexes.[16] They are readily synthesized from imidazolium ligand precursors by the addition of basic silver salts such as silver acetate, silver

[a] Institut für Anorganische Chemie, Georg-August-Universität Göttingen,
Tammannstrasse 4, 37077 Göttingen, Germany
E-mail: franc.meyer@chemie.uni-goettingen.de

Supporting information for this article is available on the WWW under http://dx.doi.org/10.1002/ejic.201100264.

carbonate or the most commonly used Ag_2O.[17–19] Often they are the first complexes that are prepared for newly developed NHC ligands in order to probe their general coordination patterns.

In this work we present a synthetic entry to new, asymmetric, pyridazine-bridged NHC/pyrazole ligand precursors (type **C**, Scheme 1). These are closely related to type **B** systems,[13] as they formally represent a switching of the positions of two adjacent C and N atoms in one of the five-membered heterocycles attached to the central pyridazine unit. However, ligands derived from **B** provide two identical organometallic $\{C^{NHC}N^{pyridazine}\}$ compartments, whereas ligands derived from **C** are quite different and will offer one organometallic $\{C^{NHC}N^{pyridazine}\}$ site and a classical (Werner-type) $\{N^{pyrazole}N^{pyridazine}\}$ site. We also report the stepwise coordination of silver(I) by the new type **C** ligand precursors, which gave rise to an interesting sequence of binding events and various structural motifs for the resulting complexes. Silver(I) complexes of the related symmetric pyridazine/pyrazole ligand **D** have been reported recently.[20]

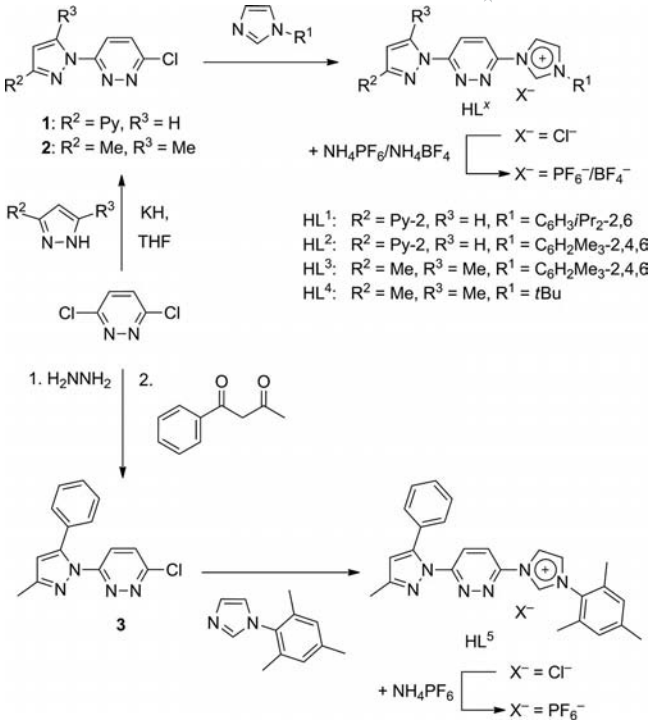

Scheme 2. Syntheses of ligand precursors $HL^{1–5}$.

Results and Discussion

A series of differently substituted pyridazine-based type **C** NHC/pyrazole ligand precursors were prepared by two general synthetic routes, starting from 3,6-dichloropyridazine (Scheme 2).[21] Addition of potassium hydride plus the appropriate pyrazole in stoichiometric amounts initially yields monosubstituted pyrazole/pyridazine compounds **1** and **2**,[22] which can then be treated with different *N*-substituted imidazoles to yield the type **C** ligand precursors. In the second step, a neat mixture of **1** or **2** and 5 equiv. of the respective imidazole is melted in an evacuated Schlenk flask; both the temperature and reaction time are crucial for obtaining good yields. The excess imidazole can be recovered by sublimation. Subsequent treatment with an aqueous solution of NH_4PF_6 or NH_4BF_4 allows exchange of the chloride for hexafluorophosphate or tetrafluoroborate anions, which impart better solubility and improved crystallization behaviour on the ligand precursors. Four ligands $HL^{1–4}$ were prepared by this route, all carrying bulky substituents (*tert*-butyl or substituted aryl) at the imidazolium ring and a 2-pyridyl group (HL^1, HL^2) or two methyl groups (HL^3, HL^4) at the pyrazole side. For ligand precursor HL^5, the pyrazole ring in the intermediate compound **3** is preferably formed by a known two-step condensation reaction[23] by sequentially adding hydrazine and 1-phenylbutane-1,3-dione to 3,6-dichloropyridazine (Scheme 2). In a subsequent step the (2,4,6-trimethylphenyl)imidazolium ring is attached by heating a neat mixture of **3** and (2,4,6-trimethylphenyl)imidazole, followed by anion exchange.

All of the ligand precursors $HL^{1–5}$ were fully characterized by elemental analysis, mass spectrometry (ESI-MS and HRMS) and NMR spectroscopy. Characteristic ^1H NMR signals for the acidic imidazolium C^2 protons (CH^{im2}) appear at high frequency in the range of δ = 9.3–9.7 ppm; these signals disappear due to H/D exchange when the spectra are recorded in CD_3OD. Also noticeable are the pyridazine protons (CH^{pdz}) in positions C^4 and C^5, which can be observed as two separate doublets with a ^3J coupling of 9.5 Hz because of the asymmetric substitution of the pyridazine.

In Figure 1 the ORTEP plots of $HL^3(PF_6)$ and $HL^2(PF_6)$ are shown as representative examples for the molecular structures of the new ligand precursors. The X-ray structures of several other ligand precursors with either hexafluorophosphate or tetrafluoroborate anions are given in the Supporting Information. In most cases the nitrogen atoms of the pyridazine point away from the imidazolium C^2 protons and from the nitrogen atoms of the pyrazoles, as is seen in $HL^3(PF_6)$. The only exception is the molecular structure of $HL^2(PF_6)$, where the imidazolium C^2 hydrogen atom and the pyridazine N atoms point in the same direction, with the pyrazole N^6 atom oriented towards the back. The planes of the pyrazole and imidazolium rings are more or less twisted (9–45°) in all of these structures, suggesting free rotation of the heterocycles. This should enable the chelating binding mode to form the desired complexes. In almost all structures the anion is located near the imidazolium C^2 proton with C···F distances of between 3.08 and 3.21 Å and C–H···F angles ranging from 139 to 176°. These values are within the usually accepted limits for such hydrogen bonds.[24] Only in the case of $HL^2(PF_6)$ do two ligand precursors form a face-to-face dimer stabilized by interactions between the pyridine N-atoms and the imidazolium C^2 protons of the opposing ligand (Figure 1). The anions are located on either side of the ligand dimer plane.

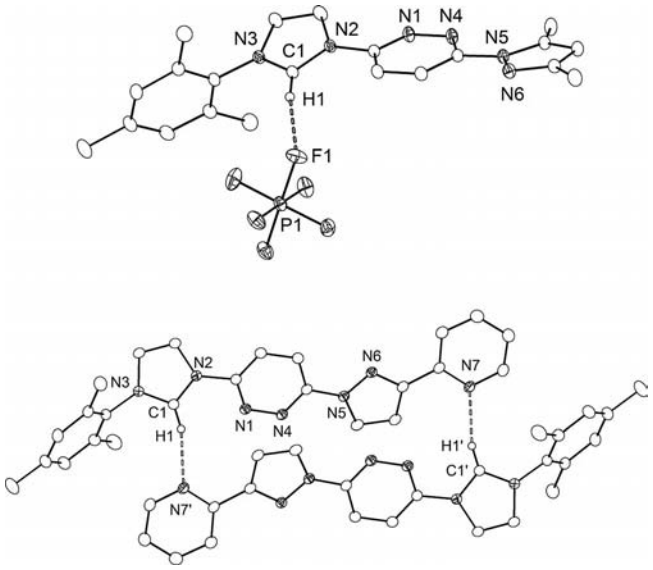

Figure 1. ORTEP plots (30% probability thermal ellipsoids) of the molecular structures of $HL^3(PF_6)$ (top) and $HL^2(PF_6)$ (bottom) emphasizing the hydrogen bonding (dashed lines). For the sake of clarity most hydrogen atoms have been omitted. Selected bond lengths [Å] and angles [°] for $HL^3(PF_6)$: C1···F1 3.101(2); C1–H1···F1 170(2), N2–C1–N3 108.6(1); for $HL^2(PF_6)$: C1···N7′ 3.188(2); C1–H1···N7′ 161(2), N2–C1–N3 108.3(2). Symmetry transformation used to generate equivalent atoms (′): 1 – *x*, 1 – *y*, 1 – *z*.

According to the method established by Lin et al.,[19] addition of Ag_2O to an MeCN or acetone solution of the respective ligand precursor allows the straightforward preparation of silver–NHC complexes (Scheme 3). In this reaction Ag_2O is used as a base that deprotonates the relatively acidic imidazolium C^2 atom. The reaction is not air- or moisture-sensitive, no additional base is needed, and the surplus Ag_2O can easily be removed by filtration. Yields are generally about 80% after 48 h of stirring at ambient temperature.

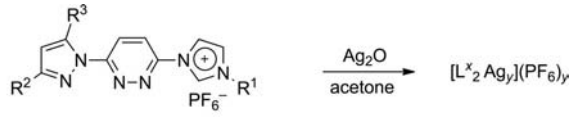

$HL^3(PF_6)$: R^2 = Me, R^3 = Me, R^1 = $C_6H_2Me_3$-2,4,6 — **4** (L^3, *y* = 1)
$HL^4(PF_6)$: R^2 = Me, R^3 = Me, R^1 = *t*Bu — **4′** (L^4, *y* = 1)
$HL^5(PF_6)$: R^2 = Me, R^3 = Ph, R^1 = $C_6H_2Me_3$-2,4,6 — **5′** (L^5, *y* = 2)

Scheme 3. Preparation of the various silver(I) complexes **4**–**5′**.

Silver(I) complexes of the type $[L_2Ag](PF_6)$ were isolated with ligands HL^3 (**4**) and HL^4 (**4′**) and have been fully characterized. They are stable as solids but slowly decompose in solution and should be stored under exclusion of light. In the ^1H NMR spectra recorded in aprotic solvents the signals for the imidazolium C^2 protons are missing, which reflects coordination of the generated carbenes. Signals for the NHC C^2 atoms in the ^{13}C NMR spectra are shifted by about 50 ppm downfield compared to those of the free ligands, from about δ = 136 to 184 ppm, in agreement with literature reports for other complexes with a linear C^{NHC}–Ag^I–C^{NHC} motif.[14b] Solid-state structures for complexes **4** and **4′** are shown in Figures 2 and 3, respectively. In both cases a single silver ion is coordinated in a linear fashion by the NHC subunits of both ligand strands. In **4**, the bond length between the NHC and the silver ion is about 2.09 Å and the C–Ag–C bond angle is close to linearity (179°). Just as in the free ligands, the pyridazine N-atoms point backwards, away from the silver ion.

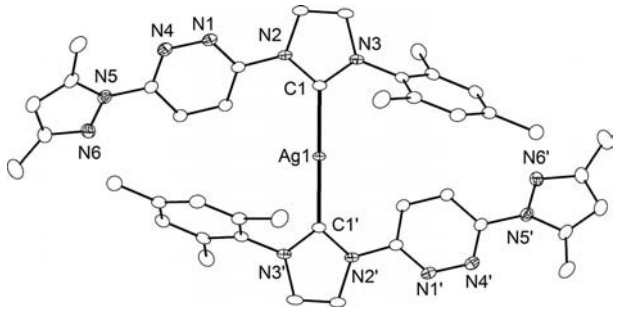

Figure 2. ORTEP plot (30% probability thermal ellipsoids) of the molecular structure of the cation of **4**. Hydrogen atoms have been omitted for clarity. Selected bond lengths [Å] and angles [°]: Ag1–C1 2.0852(15), Ag1–C1′ 2.0852(15); C1–Ag1–C1′ 179.24(8), N2–C1–N3 104.29(13). Symmetry operation used to generate equivalent atoms (′): 1 – *x*, *y*, –*z* + 1/2.

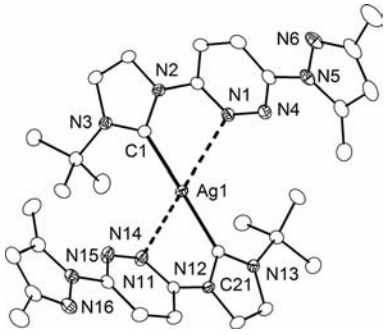

Figure 3. ORTEP plot (30% probability thermal ellipsoids) of the molecular structure of the cation of **4′**. Hydrogen atoms have been omitted for clarity. Selected bond lengths [Å] and angles [°]: Ag1–C1 2.106(3), Ag1–C21 2.104(3), Ag1–N1 2.824(3), Ag1–N14 2.819(3); C1–Ag1–C21 174.3(1), N1–Ag1–N14 126.3(1), N2–C1–N3 104.3(2), N12–C21–N13 104.3(2).

In contrast, the molecular structure of complex **4′** suggests a weak secondary interaction of the pyridazine N^1 and N^{14} atoms with the silver ion (Figure 3), as the pyridazine N atoms are orientated towards the metal atom, and the corresponding Ag···N distances are relatively short at approximately 2.82 Å. This may be the reason why the bond between the NHC and the silver ion in **4′** is slightly longer (2.15 Å) than in **4**, and the C–Ag–C angle is slightly more bent (174°).

The availability of noncoordinating pyrazole N- and pyridazine N-atoms in **4** and **4′** suggests that binding of additional silver ions should be possible under appropriate conditions. Complex **4** was thus titrated with $AgBF_4$ and the reaction mixture analyzed by ^1H NMR spectroscopy. The chemical shift of the pyrazole C^4 proton (CH^{pz4}) usu-

ally is a good indicator for the involvement of the pyrazole N-atom in metal ion binding. Figure 4 shows the changes of the chemical shift for the pyrazole C^4H signal upon addition of up to 3 equiv. of $AgBF_4$ to a solution of **4** in MeCN.[25] The slope of the curve changes after the addition of 1 equiv., and the chemical shift finally remains constant after addition of 2 equiv. This suggests the sequential formation of species $[(L^3)_2Ag_2]^{2+}$ (**6**) and $[(L^3)_2Ag_3]^{3+}$ (**7**) in solution. Both complexes were subsequently isolated as crystalline materials, and their molecular structures were determined by XRD (Figures 5 and 6, respectively).

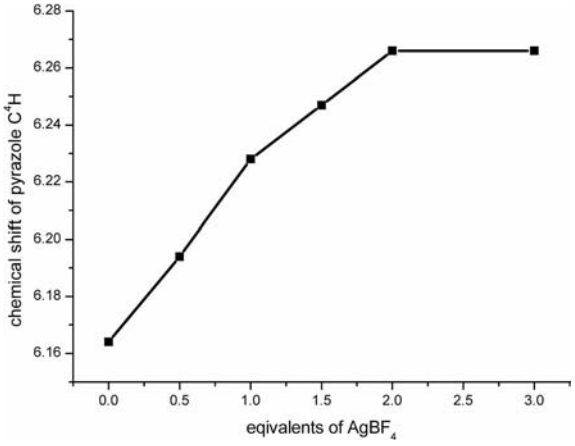

Figure 4. Changes of the ^1H NMR chemical shift of the pyrazole C^4 proton upon addition of $AgBF_4$ to a solution of **4** in MeCN.

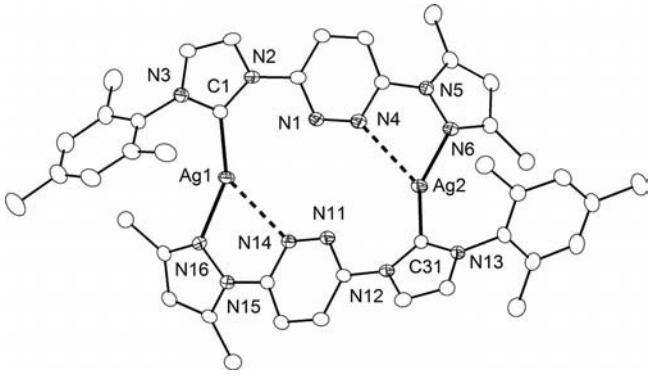

Figure 5. ORTEP plot (30% probability thermal ellipsoids) of the molecular structure of the cation of **6**. Hydrogen atoms have been omitted for clarity. Selected bond lengths [Å] and angles [°]: Ag1–C1 2.090(3), Ag1–N16 2.190(2), Ag1–N14 2.580(2), Ag2–C31 2.087(2), Ag2–N6 2.175(2), Ag2–N4 2.613(2), Ag1···Ag2 5.5828(4); C1–Ag1–N16 154.19(10), C1–Ag1–N14 133.50(9), N16–Ag1–N14 69.27(7), C31–Ag2–N6 153.40(10), C31–Ag2–N4 133.83(9), N6–Ag2–N4 68.52(8), N2–C1–N3 104.1(2), N12–C31–N13 104.2(2).

Complex **6**, which was obtained after addition of 1 equiv. of $AgBF_4$, features two antiparallel ligand strands that are held together by two silver(I) ions, each coordinated by an NHC C^2- and a pyrazole N-atom. Additional interactions between the metal ions and adjacent pyridazine N-atoms are significantly more pronounced than in **4′**, as judged from the shorter Ag···N distances (2.58 and 2.61 Å) as well as the strong deviation of the C1–Ag1–N15 and C31–Ag2–N6 axes from linearity (153 and 154°). The coordination

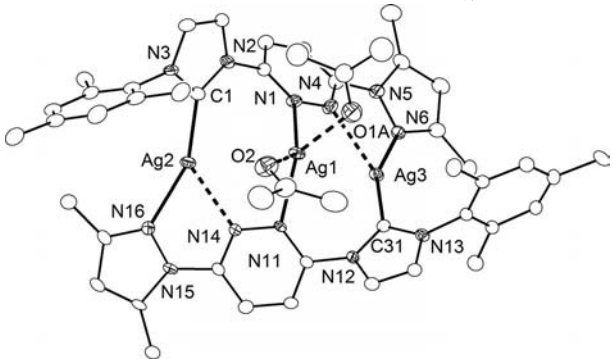

Figure 6. ORTEP plot (30% probability thermal ellipsoids) of the molecular structure of the cation of **7**. Hydrogen atoms and disordered parts have been omitted for clarity. Selected bond lengths [Å] and angles [°]: Ag1–N1 2.290(4), Ag1–N11 2.272(4), Ag1–O1A 2.322(8), Ag1–O2 2.456(5), Ag2–C1 2.103(5), Ag2–N16 2.284(5), Ag2–N14 2.422(4), Ag3–C31 2.090(5), Ag3–N6 2.266(4), Ag3–N4 2.407(5), Ag1···Ag2 3.410(1), Ag1···Ag3 3.332(1); N11–Ag1–N1 114.80(14), N11–Ag1–O1A 140.4(2), N1–Ag1–O1A 93.3(2), N11–Ag1–O2 91.05(17), N1–Ag1–O2 140.93(17), O1A–Ag1–O2 82.3(2), C1–Ag2–N16 156.97(18), C1–Ag2–N14 131.58(17), N16–Ag2–N14 69.04(15), C31–Ag3–N6 155.36(17), C31–Ag3–N4 133.92(17), N6–Ag3–N4 69.61(15), N2–C1–N3 103.2(4), N12–C31–N13 103.1(4).

environment of the metal ions is thus best described as {2 + 1}; the Ag···Ag distance is about 5.58 Å.

Addition of one more equivalent of $AgBF_4$ produces the trinuclear complex **7**, which was isolated and crystallized as the salt $[(L^3)_2Ag_3](PF_6)_2(BF_4)$ from an acetone/Et_2O solution. Its molecular structure (Figure 6) is closely related to that of **6** with two antiparallel ligand strands, but a third silver(I) ion (Ag1) is now accommodated in a central position, bound to the pyridazine N^1 and N^{11} atoms that were still available for metal ion binding in the precursor **6**. Two acetone molecules are loosely bound to Ag1 (Ag1–O1A 2.32, Ag1–O2 2.46 Å), resulting in a distorted tetrahedral coordination and an acute N1–Ag1–N11 angle of 114°. Distances between the central Ag1 and the peripheral Ag2 and Ag3 atoms are 3.41 and 3.33 Å, respectively. These distances are well above 2.9 Å, albeit shorter than the sum of the van der Waals radii (3.44 Å); we assume that d^{10}–d^{10} interactions are weak, if present at all.[26,27]

It is interesting to note that binding a second silver(I) ion to **4** and formation of dinuclear **6** requires the breaking of an Ag–C^{NHC} bond and reorganization of the ligands, as both metal ions in **6** feature a C^{NHC}–Ag–N motif. One may suggest that this process occurs by an intermediate complex **5** with parallel ligand strands, which subsequently rearranges to the thermodynamically more stable **6** (Scheme 4). Support for this assumption comes from the molecular structure of the dinuclear complex $[(L^5)_2Ag_2](PF_6)_2$ (**5′**, Figure 7), which was isolated from the reaction of HL^5 and Ag_2O in acetone.

In **5′** one of the silver ions (Ag1) still retains the C–Ag–C coordination motif from the precursor complex $[(L^5)_2Ag]^+$ {assuming that the structure for $[(L^5)_2Ag]^+$ is similar to that of **4** or **4′**}, and the second silver ion is hosted in the open $\{N_4\}$ site with two shorter Ag–$N^{pyrazole}$

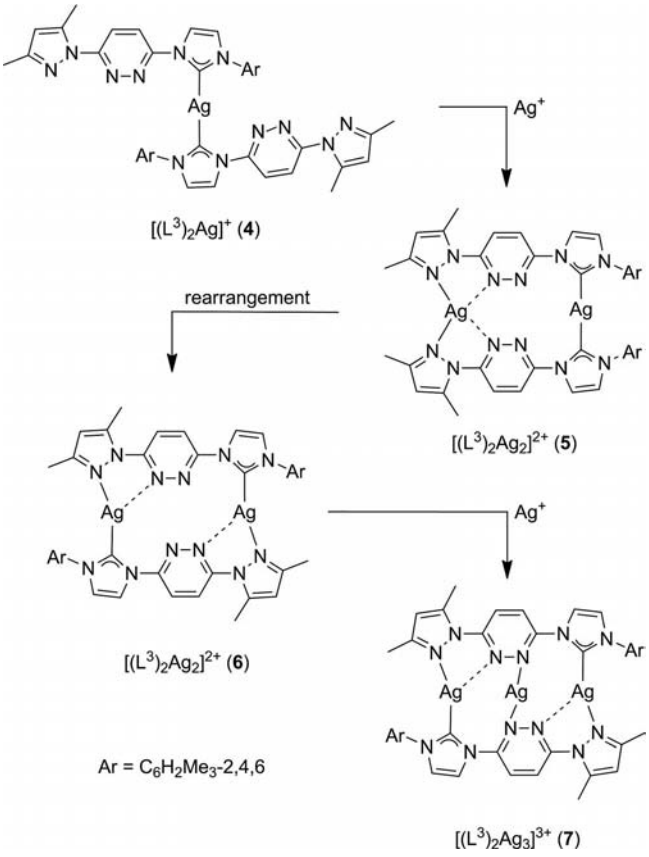

Scheme 4. Proposed sequence for the formation of **4**–**7**.

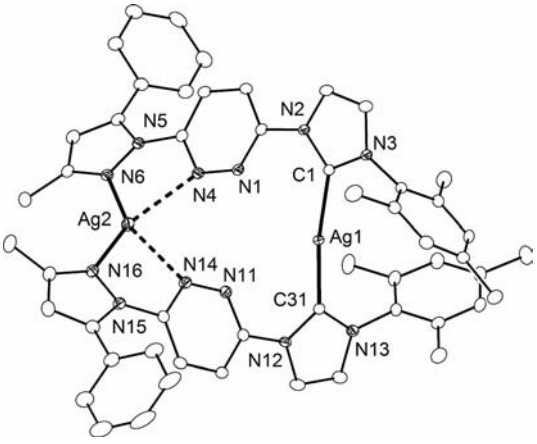

Figure 7. ORTEP plot (30% probability thermal ellipsoids) of the molecular structure of the cation of **5′**. Hydrogen atoms have been omitted for clarity. Selected bond lengths [Å] and angles [°]: Ag1–C1 2.080(2), Ag1–C31 2.077(2), Ag2–N6 2.2105(18), Ag2–N16 2.2424(19), Ag2–N14 2.5065(19), Ag2–N4 2.5971(19), Ag1···Ag2 5.4269(3); C1–Ag1–C31 170.90(8), N6–Ag2–N16 138.03(7), N6–Ag2–N14 150.10(6), N16–Ag2–N14 69.18(6), N6–Ag2–N4 67.35(6), N16–Ag2–N4 152.73(6), N14–Ag2–N4 89.65(6), N2–C1–N3 104.2(2), N12–C31–N13 103.8(2).

bonds (2.21/2.24 Å) and two longer Ag–$N^{pyridazine}$ bonds (2.51/2.60 Å). The distance between the metal ions is about 5.43 Å without any direct interaction between them.

However, the proposed intermediate **5** was not detected during the reaction of **4** to **6**, and the conversion of **5′** to a rearranged product was not observed by NMR spectroscopy (see below). It is likely that the putative rearrangement **5** → **6** does not proceed by simple dissociation, rotation and rebinding of one of the ligands, but by a more complex reaction sequence that may even be an intermolecular process. Some indication for this can be seen in the molecular structure of the trinuclear complex $[(L^3)_3Ag_3]^{3+}$ (**8**), which has the same ligand/metal ratio as in **5** and **6** (1:1). Only a few crystals of this compound were obtained by crystallization from an acetone/Et_2O solution in one experiment, and the moderate quality of its crystallographic structure determination does not permit any detailed discussion of metric parameters. However, the overall structure is revealed (Figure 8) and features three silver atoms in distinct coordination environments, namely C^{NHC}–Ag–C^{NHC}, C^{NHC}–Ag–$N^{pyrazole}$, and $N^{pyrazole}$–Ag–$N^{pyrazole}$ (all with additional weak $N^{pyridazine}$–Ag interactions). Complex **8** may thus be viewed as a potential intermediate of the multistep ligand reshuffling process from **5** to **6**. These interconversions likely involve various oligonuclear species and are rapid on the NMR time scale.

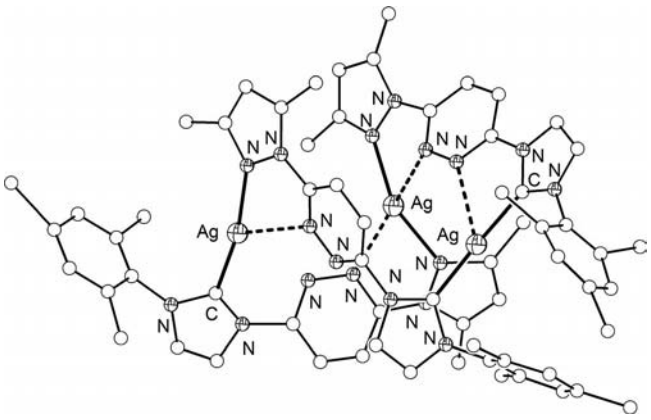

Figure 8. Plot of the molecular structure of the cation of **8**. Hydrogen atoms have been omitted for clarity.

Characterization of the multinuclear silver complexes by NMR spectroscopy and ESI mass spectrometry is hampered by rapid dynamic processes and the presence of multiple species in solution. In all cases the ion $[L_2Ag]^+$ represents the major signal in the ESI mass spectra (acetone solution), although the ion $[LAg]^+$ is also detected.

Room-temperature ^1H NMR spectra of **4** feature sharp signals in $[D_3]$MeCN, which are broadened in $[D_6]$acetone. Upon cooling of a solution in $[D_6]$acetone to 233 K the resonances split into two major and several minor sets, which may tentatively be assigned to different rotational isomers with one or both pyridazine groups pointing their N atoms towards or away from the metal ion (as reflected by the structures of **4** and **4′** in the solid state). ^{13}C NMR spectroscopy reveals just two doublets for C^2 at low temperature {233 K, $[D_6]$acetone: δ = 182.6 ppm, $^1J(^{13}C^{107}Ag)$ = 182.5 Hz, $^1J(^{13}C^{109}Ag)$ = 203.8 Hz} and a broadened resonance at room temperature. The ESI mass spectrum of **4**

only shows the dominant signals for $[(L^3)_2Ag]^+$ and $[(L^3)Ag]^+$, besides some free ligand $[L^3]^+$.

When a solution of **4** in $[D_6]$acetone is treated with 1 equiv. of $AgBF_4$ at 233 K, a single set of resonances is discernible in the ^1H NMR spectrum that is identical to the spectrum obtained by dissolving crystals of **6** in the same solvent. This suggests that reshuffling of the ligands is rapid even at low temperature and that the intermediate **5** cannot be detected for this particular ligand scaffold, L^3. In the ESI mass spectrum of **6** (acetone solution) the ions $[(L^3)_2Ag]^+$ and $[(L^3)Ag]^+$ again give rise to the most intense signals, but $[(L^3)_2Ag_2]^+$ (3% intensity) and $[(L^3)_2Ag_2(PF_6)]^+$ (6%) are also observed. ^1H NMR spectra of the related **5′** show relatively strong solvent dependence, yet only a single set of signals is seen in both CD_3CN and $[D_6]$acetone. Basically the same spectrum is observed upon dissolving crystals of **5′** in $[D_6]$acetone at low temperature (233 K) although the chemical shifts undergo some reversible changes upon warming to 318 K. A 1:1 mixture of **5′** and **6** in $[D_6]$acetone shows several signal sets in the ^1H NMR spectrum (including those for the parent compounds) as well as ESI-MS peaks for, among others, $[(L^3)_2Ag]^+$, $[(L^3)(L^5)Ag]^+$ and $[(L^5)_2Ag]^+$. This confirms that rapid ligand scrambling occurs in solution. In line with this conclusion, compounds **6** and **8** show very similar ESI mass spectra, and $[(L^3)_3Ag_2(PF_6)]^+$ is detected as a minor signal (<1%). ^1H diffusion ordered spectroscopy (DOSY) experiments reveal that **6** and **7** have similar diffusion coefficients, in accordance with the similar radii of the complexes $[(L^3)_2Ag_2]^{2+}$ and $[(L^3)_2Ag_3]^{3+}$. We assume that the central third Ag^+ ion is only weakly bound by the two pyridazine N atoms in **7**.

Conclusions

Members of the new family of ligand precursors $HL^{1–5}$ with different diazole rings attached to both the 3- and 6-positions of a central pyridazine core, namely a pyrazole and an imidazolium group, offer two topologically similar yet electronically distinct potential binding compartments, complemented by the hemilabile pyridazine N-atom of the bridge. Upon treatment with Ag_2O sequential coordination of up to three silver(I) ions is observed. It starts at the organometallic NHC site, yielding species $[L_2Ag]^+$ with two ligand strands attached by their carbene C^2 atoms. Coordination of a second Ag^+ ion to the classical pyrazole N-site may induce ligand reshuffling to give antiparallel ligand strands and a mixed {C/N} coordination of both metal ions, although this seems to depend on the peripherial ligand substituents. A third Ag^+ ion can be accommodated by two of the central pyridazine N atoms, but is just loosely bound. The systems appear to be labile in solution, with multiple species and several rotational isomers detected by ESI mass spectrometry and low-temperature NMR spectroscopy. We assume that the hemilabile character of the pyridazine N-atom and its temporary involvement in metal ion binding, as reflected by some of the crystal structures, contributes to fluxional processes. Transmetallation of the silver complexes may give rise to interesting pyridazine-bridged homo- and heterodimetallic complexes, and is currently under investigation.

Experimental Section

General: Compounds **1**,[22] **2**[22] and **3**[23] were synthesized according to the published procedures with slight modifications. All other reagents were purchased from commercial sources and employed without further treatment. Melting points were determined with an OptiMelt system (Stanford Research Systems, Inc.) by using open capillaries, and values are uncorrected. ^1H and ^{13}C NMR spectra were recorded with Bruker Avance 300 and Bruker Avance 500 spectrometers. ^{13}C resonances were obtained with broad-band proton decoupling, and spectra were recorded at 298 or 233 K. ^1H and ^{13}C NMR chemical shifts were referenced internally to solvent signals. ESI mass spectra were recorded by using an Applied Biosystems API 2000. HRMS measurements were recorded with a Bruker FTICR-MS APEX IV. IR spectra from KBr pellets were recorded with a Digilab Excalibur Series FTS 3000 spectrometer. Elemental analyses were performed at the analytical laboratory of the Institute for Inorganic Chemistry at the Georg August University by using an Elementar Vario EL III instrument. Details of the X-ray crystallographic determinations can be found in the Supporting Information. CCDC-806607 [for $HL^1(PF_6)$], -806608 [for $HL^2(PF_6)$], -806609 [for $HL^3(PF_6)$], -806610 [for $HL^4(BF_4)$], -806611, [for $HL^5(PF_6)$], -806612 (for **4**), -806613 (for **4′**), -806614 (for **5′**), -806615 (for **6**) and -806616 (for **7**) contain the supplementary crystallographic data for this paper. These data can be obtained free of charge from The Cambridge Crystallographic Data Centre via www.ccdc.cam.ac.uk/data_request/cif.

3-[3-(2,6-Diisopropylphenyl)-3*H*-imidazolium-1-yl]-6-(3-pyridin-2-yl-pyrazol-1-yl)pyridazine Tetrafluoroborate [$HL^1(BF_4)$]: A neat mixture of **3** (1.50 g, 5.82 mmol) and 1-(2,6-diisopropylphenyl)-1*H*-imidazole (6.65 g, 29.1 mmol) was heated in an evacuated flask at 150 °C for 48 h. The residue was dissolved in MeOH (30 mL) and poured into Et_2O (800 mL). The excess imidazole was recycled from the organic phase. A brownish residue was collected by filtration, dissolved in H_2O (30 mL) and MeCN (30 mL) and stirred with NH_4BF_4 (1.23 g, 11.7 mmol) for 2 h. The solvent was removed under reduced pressure and the residue was again dissolved in MeCN (50 mL). HL^1 (2.15 g, 3.85 mmol, 66%) was obtained as a pale brown powder after filtration and removal of the solvent. Crystallization by slow diffusion of diethyl ether into an MeCN solution of the crude product at room temperature afforded colourless crystals. M.p. 252 °C. $C_{27}H_{28}BF_4N_7$ (537.23): calcd. C 60.35, H 5.25, N 18.25; found C 59.94, H 5.31, N 18.03. IR (KBr): $\tilde{\nu}$ = 3431 (w, br.), 3153 (w), 2968 (w), 2932 (w), 2873 (vw), 1591 (w), 1538 (m), 1483 (m), 1456 (s), 1429 (w), 1367 (m), 1325 (vw), 1284 (w), 1059 (vw), 1027 (w), 943 (w), 843 (s), 772 (w), 558 (m) cm^{-1}. ^1H NMR (300 MHz, CD_3CN): δ = 1.20 (d, ^3J = 6.8 Hz, 6 H, $CH_3{}^{i\text{pr}}$), 1.22 (d, ^3J = 6.8 Hz, 6 H, $CH_3{}^{i\text{pr}}$), 2.52 (sept, ^3J = 6.8 Hz, 2 H, $CH^{i\text{pr}}$), 7.24 (d, ^3J = 2.8 Hz, 1 H, CH^{pz4}), 7.39 (ddd, ^3J = 7.5 Hz, ^3J = 4.9 Hz, ^4J = 1.2 Hz 1 H, CH^{py5}), 7.48 (d, ^3J = 7.8 Hz, 2 H, $CH^{\text{ar3,5}}$), 7.64 (t, ^3J = 7.8 Hz, 1 H, CH^{ar4}), 7.85 (t, ^3J = 1.9 Hz, 1 H, CH^{im4}), 7.88 (dt, ^3J = 7.8 Hz, ^4J = 1.8 Hz, 1 H, CH^{py4}), 8.17 (d, ^3J = 7.8 Hz, 1 H, CH^{py3}), 8.31 (d, ^3J = 9.5 Hz, 1 H, CH^{pdz}), 8.50 (t, ^3J = 1.9 Hz, 1 H, CH^{im5}), 8.64 (ddd, ^3J = 4.9 Hz, ^3J = 1.8 Hz, ^4J = 1 Hz, 1 H, CH^{py6}), 8.66 (d, ^3J = 9.5 Hz, 1 H, CH^{pdz}), 8.84 (d, ^3J = 2.8 Hz, 1 H, CH^{pz5}), 9.66 (t, ^3J = 1.9 Hz, 1 H, CH^{im2}) ppm. ^{13}C NMR (75 MHz, CD_3CN): δ = 24.3 ($CH_3{}^{i\text{pr}}$), 24.5

(CH_3^{ipr}), 29.5 (C^{ipr}), 109.5 (C^{pz4}), 121.6 (C^{py3}), 121.7 (C^{im5}), 122.2 (C^{pdz}), 124.0 (C^{pdz}), 125.0 (C^{py5}), 125.8 ($C^{ar3,5}$), 127.3 (C^{im4}), 130.5 (C^{pz5}), 131.1 (C^{ar1}), 133.2 (C^{ar4}), 136.2 (C^{im2}), 138.5 (C^{py4}), 146.5 ($C^{ar2,6}$), 150.5 (C^{py6}), 150.8 (C^{Pdz}), 151.5 (C^{py2}), 156.6 (C^{pz3}), 156.6 (C^{pdz}) ppm. MS (ESI^+): *m/z* (%) = 450.2 (100) $[M - BF_4]^+$. MS (ESI^-): *m/z* (%) = 87.0 (100) $[BF_4]^-$. HRMS (ESI^+): calcd. for $C_{27}H_{28}N_7$ 450.2401; found 450.2399.

3-(3-Pyridin-2-ylpyrazol-1-yl)-6-[3-(2,4,6-trimethylphenyl)-3*H*-imidazolium-1-yl]pyridazine Hexafluorophosphate [$HL^2(PF_6)$]: A neat mixture of **3** (1.50 g, 5.82 mmol) and 2,4,6-trimethylphenyl-1*H*-imidazole (5.42 g, 29.1 mmol) was heated in an evacuated flask at 150 °C for 48 h. The residue was dissolved in MeOH (30 mL) and poured into Et_2O (800 mL). The excess imidazole was recycled from the organic phase. The brownish residue was collected by filtration and dissolved in H_2O (30 mL) and MeCN (30 mL) and stirred with NH_4PF_6 (1.89 g, 11.6 mmol) for 2 h. The solvent was removed under reduced pressure, and the residue was again dissolved in MeCN (60 mL). HL^2 (2.08 g, 4.20 mmol, 72%) was obtained as a pale brown powder after removal of the solvent. Crystallization by slow diffusion of diethyl ether into an MeOH solution of the crude product at room temperature afforded colourless crystals. M.p. 267 °C. $C_{24}H_{22}F_6N_7P$ (553.16): calcd. C 52.08, H 4.01, N 17.72; found C 52.37, H 3.65, N 17.99. IR (KBr): $\tilde{\nu}$ = 3426 (w, br), 3165 (w), 3143 (w), 3091 (w), 3017 (w), 2924 (vw), 1586 (m), 1554 (m), 1542 (m), 1485 (m), 1457 (s), 1372 (m), 1253 (w), 1057 (w), 961 (vw), 944 (w), 855 (s), 831 (s), 778 (m), 558 (m) cm^{-1}. ^1H NMR (300 MHz, CD_3CN): δ = 2.15 (s, 6 H, $CH_3^{ar2,6}$), 2.39 (s, 3 H, CH_3^{ar4}), 7.17 (s, 2 H, $CH^{ar3,5}$), 7.24 (d, ^3J = 2.8 Hz, 1 H, CH^{pz4}), 7.36 (ddd, ^3J = 7.5 Hz, ^3J = 4.8 Hz, ^4J = 1.2 Hz, 1 H, CH^{py5}), 7.76 (t, ^3J = 1.7 Hz, 1 H, CH^{im4}), 7.89 (dt, ^3J = 7.5 Hz, ^4J = 1.8 Hz, 1 H, CH^{py4}), 8.16 (dt, ^3J = 8 Hz, ^4J = 1.1 Hz, 1 H, CH^{py3}), 8.24 (d, ^3J = 9.5 Hz, 1 H, CH^{pdz}), 8.46 (t, ^3J = 1.7 Hz, 1 H, CH^{im5}), 8.64 (ddd, ^3J = 4.8 Hz ^3J = 1.8 Hz, ^4J = 1.1 Hz 1 H, CH^{py6}), 8.66 (d, ^3J = 9.5 Hz, 1 H, CH^{pdz}), 8.84 (d, ^3J = 2.8 Hz, 1 H, CH^{pz5}), 9.55 (t, ^3J = 1.7 Hz, 1 H, CH^{im2}) ppm. ^{13}C NMR (75 MHz, CD_3CN): δ = 17.7 ($CH_3^{ar2,6}$), 21.3 (CH_3^{ar4}), 109.5 (C^{pz4}), 121.4 (C^{py3}), 121.5 (C^{im5}), 122.3 (C^{pdz}), 123.9 (C^{pdz}), 124.9 (C^{py5}), 126.5 (C^{im4}), 130.6 (C^{pz5}), 130.7 ($C^{ar3,5}$), 131.8 (C^{ar1}), 135.8 ($C^{ar2,6}$), 136.2 (C^{im2}), 138.2 (C^{py4}), 142.8 (C^{ar4}), 150.7 (C^{py6}), 150.7 (C^{pdz}), 151.7 (C^{py2}), 156.6 (C^{pz3}), 156.9 (C^{pdz}) ppm. MS (ESI^+): *m/z* (%) = 408.1 (100) $[M - PF_6]^+$. MS (ESI^-): *m/z* (%) = 144.9 (100) $[PF_6]^-$. HRMS (ESI^+): calcd. for $C_{24}H_{22}N_7$ 408.1931; found 408.1933.

3-(3,5-Dimethylpyrazol-1-yl)-6-[3-(2,4,6-trimethylphenyl)-3*H*-imidazolium-1-yl]pyridazine Hexafluorophosphate [$HL^3(PF_6)$]: A solution of **1** (2.00 g, 9.60 mmol) and 2,4,6-trimethylphenyl-1*H*-imidazole (8.92 g, 47.9 mmol) was heated in an evacuated flask at 150 °C for 48 h. The residue was dissolved in MeOH (50 mL) and poured into Et_2O (1 L). The excess imidazole was recycled from the organic phase. The white-yellow residue was collected by filtration and dissolved in H_2O (50 mL) and MeCN (30 mL) and stirred with NH_4PF_6 (3.13 g, 19.2 mmol) for 2 h. The solvent was then removed under reduced pressure, and the residue was dissolved in MeCN (80 mL). HL^3 (3.15 g, 7.98 mmol, 83%) was obtained as a white powder after removal of the solvent. Crystallization by slow diffusion of diethyl ether into an MeCN solution of the crude product at room temperature afforded colourless crystals. M.p. 271 °C. $C_{21}H_{23}F_6N_6P$ (504.16): calcd. C 50.00, H 4.60, N 16.66; found C 49.69, H 4.47, N, 16.48. IR (KBr): $\tilde{\nu}$ = 3431 (w, br.), 3155 (w), 2976 (vw), 2929 (w), 1589 (w), 1570 (m), 1555 (m), 1481 (m), 1450 (s), 1406 (w), 1384 (w), 1361 (w), 1334 (w), 1245 (w), 1124 (w), 1032 (w), 973 (w), 842 (s), 738 (w), 558 (m) cm^{-1}. ^1H NMR (300 MHz, CD_3CN): δ = 2.14 (s, 6 H, $CH_3^{ar2,6}$), 2.28 (s, 3 H, CH_3^{pz3}), 2.38 (s, 3 H, CH_3^{ar4}), 2.72 (s, 3 H, CH_3^{pz5}), 6.21 (s, 1 H, CH^{pz4}), 7.17 (s, 2 H, $CH^{ar3,5}$), 7.74 (t, ^3J = 1.7 Hz, 1 H, CH^{im4}), 8.15 (d, ^3J = 9.5 Hz, 1 H, CH^{pdz}), 8.44 (t, ^3J = 1.7 Hz, 1 H, CH^{im5}), 8.48 (d, ^3J = 9.5 Hz, 1 H, CH^{pdz}), 9.51 (t, ^3J = 1.7 Hz, 1 H, CH^{im2}) ppm. ^{13}C NMR (75 MHz, CD_3CN): δ = 13.9 (CH_3^{pz3}), 15.4 (CH_3^{pz5}), 17.7 ($CH_3^{ar2,6}$), 21.3 (CH_3^{ar4}), 112.1 (C^{pz4}), 121.6 (C^{im5}), 123.3 (C^{pdz}), 124.6 (C^{pdz}), 126.5 (C^{im4}), 130.7 ($C^{ar3,5}$), 131.9 (C^{ar1}), 135.8 ($C^{ar2,6}$), 136.1 (C^{im2}), 142.8 (C^{ar4}), 144.0 (C^{pz5}), 149.7 (C^{pdz}), 153.4 (C^{pz3}), 158.9 (C^{pdz}) ppm. MS (ESI^+): *m/z* (%) = 359.3 (100) $[M - PF_6]^+$. MS (ESI^-): *m/z* (%) = 144.9 (100) $[PF_6]^-$. HRMS (ESI^+): calcd. for $C_{21}H_{23}N_6$ 359.1979; found 359.1980.

3-(3-*tert*-Butyl-3*H*-imidazolium-1-yl)-6-(3,5-dimethylpyrazol-1-yl)-pyridazine Tetrafluoroborate [$HL^4(BF_4)$]: A solution of **1** (1.00 g, 2.60 mmol) and 1-*tert*-butyl-1*H*-imidazole (1.62 g, 13.0 mmol) was heated in an evacuated flask at 140 °C for 48 h. The residue was dissolved in MeOH (20 mL) and poured into Et_2O (600 mL). The excess imidazole was recycled from the organic phase. The white-yellow residue was collected by filtration and dissolved in H_2O (25 mL) and MeCN (25 mL) and stirred with NH_4BF_4 (0.55 g, 5.20 mmol) for 2 h. The solvent was removed under reduced pressure, and the residue was dissolved in MeCN (20 mL). HL^4 (0.68 g, 1.77 mmol, 68%) was obtained as a white powder after removal of the solvent. Crystallization by slow diffusion of diethyl ether into an MeOH solution of the crude product at room temperature afforded colourless crystals. M.p. 203 °C. $C_{16}H_{21}BF_4N_6$ (384.18): calcd. C 50.02, H 5.51, N, 21.88; found C 49.30, H 5.29, N 21.94. IR (KBr): $\tilde{\nu}$ = 3425 (m, br.), 3169 (m), 3143 (m), 3107 (m), 2987 (m), 2933 (w), 2873 (w), 1591 (m), 1573 (m), 1556 (s), 1479 (s), 1450 (s), 1416 (m), 1380 (m), 1364 (m), 1335 (w), 1270 (w), 1219 (m), 1054 (vs), 972 (m), 842 (m), 807 (m), 739 (w), 657 (w), 525 (w) cm^{-1}. ^1H NMR (300 MHz, CD_3OD): δ = 1.72 (s, 9 H, CH_3^{tbu}), 2.24 (s, 3 H, CH_3^{pz3}), 2.70 (s, 3 H, CH_3^{pz5}), 6.19 (s, 1 H, CH^{pz4}), 7.84 (pseudo-t, ^3J = 2.1 Hz, 1 H, CH^{im4}), 8.15 (d, ^3J = 9.5 Hz, 1 H, CH^{pdz}), 8.25 (pseudo-t, ^3J = 2.1 Hz, 1 H, CH^{im5}), 8.42 (d, ^3J = 9.5 Hz, 1 H, CH^{pdz}), 9.32 (pseudo-t, ^3J = 1.9 Hz, 1 H, CH^{im2}) ppm. ^{13}C NMR (75 MHz, CD_3OD): δ = 13.8 (CH_3^{pz3}), 15.2 (CH_3^{pz5}), 29.5 (CH_3^{tbu}), 61.4 (C^{tbu}), 111.8 (C^{pz4}), 121.0 (C^{im5}), 122.4 (C^{im4}), 123.2 (C^{pdz}), 124.6 (C^{pdz}), 133.8 (C^{im2}) 143.8 (C^{pz5}), 149.6 (C^{pdz}), 153.2 (C^{pz3}), 158.6 (C^{pdz}) ppm. MS (ESI^+): *m/z* (%) = 297.3 (35) $[M - BF_4]^+$, 241.2 (100) $[M - BF_4 - tBu]^+$. MS (ESI–): *m/z* (%) = 87.0 (100) $[BF_4]^-$. HRMS (ESI^+): calcd. for $C_{16}H_{21}N_6$ 297.1822; found 297.1828.

3-(3-Methyl-5-phenylpyrazol-1-yl)-6-[3-(2,4,6-trimethylphenyl)-3*H*-imidazolium-1-yl]pyridazine Hexafluorophosphate [$HL^5(PF_6)$]: A solution of **2** (1.58 g, 5.84 mmol) and 2,4,6-trimethylphenyl-1*H*-imidazole (5.42 g, 29.1 mmol) was heated in an evacuated flask at 150 °C for 48 h. The residue was dissolved in MeOH (30 mL) and poured into Et_2O (800 mL). The excess imidazole was recycled from the organic phase. The white-yellow residue was collected by filtration and dissolved in H_2O (30 mL) and MeCN (30 mL) and stirred with NH_4PF_6 (1.90 g, 11.7 mmol) for 2 h. The solvent was removed under reduced pressure, and the residue was again dissolved in MeCN (50 mL). HL^5 (2.65 g, 4.67 mmol, 80%) was obtained as a white powder after solvent removal. Crystallization by slow diffusion of diethyl ether into an MeCN solution of the crude product at room temperature afforded colourless crystals. M.p. 243 °C. $C_{26}H_{25}F_6N_6P$ (566.18): calcd. C 55.13, H 4.45, N 14.84; found C 55.71, H 4.29, N 15.18. IR (KBr): $\tilde{\nu}$ =3434 (m, br.), 3190 (w), 3155 (w), 2964 (w), 1584 (w), 1554 (m), 1499 (w), 1464 (m), 1390 (w), 1359 (w), 1333 (w), 1260 (s), 1194 (w), 1098 (s), 1059 (m), 1026 (m), 969 (w), 841 (s), 828 (s), 760 (m), 698 (w), 558 (m) cm^{-1}. ^1H NMR (300 MHz, CD_3CN): δ = 2.10 (s, 6 H, $CH_3^{ar2,6}$), 2.36 (s, 3 H, CH_3^{ar4}), 2.37 (s, 3 H, CH_3^{pz3}), 6.50 (s, 1 H, CH^{pz4}), 7.14 (s, 2 H, $CH^{ar3,5}$), 7.36 (m, 5 H, CH^{ph}), 7.69 (pseudo-t, ^3J = 1.7 Hz, 1

H, CH^{im4}), 8.17 (d, ^3J = 9.5 Hz, 1 H, CH^{pdz}), 8.36 (pseudo-t, ^3J = 1.7 Hz, 1 H, CH^{im5}), 8.38 (d, ^3J = 9.5 Hz, 1 H, CH^{pdz}), 9.43 (pseudo-t, ^3J = 1.7 Hz, 1 H, CH^{im2}) ppm. ^{13}C NMR (75 MHz, CD_3CN): δ = 13.8 (CH_3^{pz3}), 17.5 ($CH_3^{ar2,6}$), 21.2 (CH_3^{ar4}), 112.4 (C^{pz4}), 121.5 (C^{im5}), 123.3 (C^{pdz4}), 126.4 (C^{im4}), 126.7 (C^{pdz5}), 129.4 ($C^{ph2,6}$), 129.5 (C^{ph4}), 129.6 ($C^{ph3,5}$), 130.6 ($C^{ar3,5}$), 131.7 (C^{ar1}), 132.2 (C^{ph1}), 135.6 ($C^{ar2,6}$), 136.1 (C^{im2}), 142.7 (C^{ar4}), 146.5 (C^{pz5}), 150.2 (C^{pdz}), 153.7 (C^{pz3}), 158.0 (C^{pdz}) ppm. MS (ESI^+): *m/z* (%) = 421.0 (100) $[M - PF_6]^+$. MS (ESI^-): *m/z* (%) = 144.9 (100) $[PF_6]^-$. HRMS (ESI^+): calcd. for $C_{26}H_{25}N_6$ 421.2135; found 421.2134.

General Procedure for the Preparation of the Silver Complexes $[(L^x)_2Ag](PF_6)$ and $[(L^x)_2Ag_2](PF_6)_2$: A solution of the ligand precursor $[HL^x](PF_6)$ (2.0 equiv.) in MeCN or acetone was treated with Ag_2O (2.2 equiv.), and the mixture was stirred at room temperature in the absence of light for 48 h. After addition of activated carbon, the reaction mixture was slowly filtered through Celite 545 to remove unreacted Ag_2O, yielding a clear solution. After the removal of the solvent under reduced pressure, the product was obtained. Crystals suitable for XRD analysis were grown by slow diffusion of diethyl ether into a solution of the crude product in either acetone or MeCN at room temperature.

Complex $[(L^3)_2Ag](PF_6)$ (4): Reaction of $[HL^3](PF_6)$ (1.34 g, 2.66 mmol) according to the general procedure yielded 1.27 g (1.31 mmol, 98%) of **4**. Crystallization by slow diffusion of diethyl ether into an acetone solution of $[(L^3)_2Ag](PF_6)$ at room temperature afforded colourless crystals. M.p. 178 °C. $C_{42}H_{44}AgF_6N_{12}P$ (969.21): calcd. C 52.02, H 4.57, N 17.33; found C 51.79, H 4.64, N 17.27. IR (KBr): $\tilde{\nu}$ = 3441 (m, br.), 3180 (m), 2966 (m), 2927 (m), 1582 (m), 1559 (m), 1443 (s), 1397 (m), 1354 (w), 1265 (vw), 1034 (vw), 842 (s), 739 (m), 558 (m) cm^{-1}. ^{1}H NMR (500 MHz, CD_3CN): δ = 1.86 (s, 6 H, $CH_3^{ar2,6}$), 2.24 (s, 3 H, CH_3^{pz3}), 2.36 (s, 3 H, CH_3^{ar4}), 2.61 (s, 3 H, CH_3^{pz5}), 6.18 (s, 1 H, CH^{pz4}), 6.99 (s, 2 H, $CH^{ar3,5}$), 7.37 (d, ^3J = 2.0 Hz, 1 H, CH^{im4}), 8.08 (t, ^3J = 2.0 Hz, 1 H, CH^{im5}), 8.19 (d, ^3J = 9.5 Hz, 1 H, CH^{pdz}), 8.24 (d, ^3J = 9.5 Hz, 1 H, CH^{pdz}) ppm. ^{13}C NMR (125 MHz, CD_3CN): δ = 14.0 (CH_3^{pz3}), 15.1 (CH_3^{pz5}), 17.8 ($CH_3^{ar2,6}$), 21.3 (CH_3^{ar4}), 111.7 (C^{pz4}), 121.7 (C^{im5}), 124.2 (C^{pdz}), 124.7 (C^{pdz}), 125.6 (C^{im4}), 130.3 ($C^{ar3,5}$), 135.8 ($C^{ar2,6}$), 136.7 (C^{ar1}), 140.7 (C^{ar4}), 143.7 (C^{pz5}), 153.1 (C^{pz3}), 153.8 (C^{pdz}), 157.7 (C^{pdz}), 183.3 (C^{im2}) ppm. MS (ESI^+): *m/z* (%) = 825.3 (100) $[L_2Ag]^+$. MS (ESI^-): *m/z* (%) = 144.9 (100) $[PF_6]^-$. HRMS (ESI^+): calcd. for $C_{42}H_{44}AgN_{12}$ 823.2857; found 823.2860.

Complex $[(L^4)_2Ag](PF_6)$ (4′): Reaction of $[HL^4](PF_6)$ (300 mg, 0.68 mmol) according to the general procedure yielded 237 mg (0.28 mmol, 82%) of the crude product $[(L^3)_2Ag](PF_6)$. The ^{1}H NMR spectrum shows an impurity of ca. 10% free ligand. Crystallization by slow diffusion of diethyl ether into an acetone solution of the crude product at room temperature afforded colourless crystals. IR (KBr): $\tilde{\nu}$ = 3669 (w), 3588 (w), 3442 (w, br.), 3192 (w), 3160 (m), 2981 (m), 2935 (w), 1623 (w), 1583 (m), 1555 (m), 1468 (s), 1449 (s), 1383 (m), 1371 (m), 1332 (m), 1294 (w), 1240 (m), 1218 (w), 1058 (m), 956 (w), 847 (s, br.), 738 (m), 609 (w), 558 (s) cm^{-1}. ^{1}H NMR (300 MHz, CD_3CN): δ = 1.79 (s, 9 H, CH_3^{tbu}), 2.29 (s, 3 H, CH_3^{pz3}), 2.46 (s, 3 H, CH_3^{pz5}), 6.23 (s, 1 H, CH^{pz4}), 7.64 (d, ^3J = 2.1 Hz, 1 H, CH^{im4}), 7.70 (d, ^3J = 2.1 Hz, 1 H, CH^{im5}), 8.06 (d, ^3J = 9.5 Hz, 1 H, CH^{pdz}), 8.10 (d, ^3J = 9.5 Hz, 1 H, CH^{pdz}) ppm. ^{13}C NMR (75 MHz, CD_3CN): δ = 14.4 (CH_3^{pz3}), 14.7 (CH_3^{pz5}), 31.8 (CH_3^{tbu}), 59.9 (C^{tbu}), 112.0 (C^{pz4}), 120.2 (C^{im5}), 122.6 (C^{im4}), 124.6 (C^{pdz}), 125.3 (C^{pdz}), 144.1 (C^{pz5}), 153.6 (C^{pz3}), 154.7 (C^{pdz}), 156.3 (C^{pdz}), 180.4 (^{im2}) ppm. MS (ESI^+): *m/z* (%) = 699.3 (100) $[L_2Ag]^+$. MS (ESI^-): *m/z* (%) = 144.9 (100) $[PF_6]^-$. HRMS (ESI^+): calcd. for $C_{32}H_{40}AgN_{12}$ 699.2544; found 699.2545.

Complex $[(L^5)_2Ag_2](PF_6)$ (5′): Reaction of $[HL^5](PF_6)$ (600 mg, 1.06 mmol) according to the general procedure yielded 495 mg (0.45 mmol, 85%) of **5′**. Crystallization by slow diffusion of diethyl ether into an acetone solution of the crude product at room temperature afforded colourless crystals of the composition $[(L^5)_2Ag_2](PF_6)_2$. M.p. 186 °C. Elemental analysis suggests, however, that the bulk material is $[(L^5)_2Ag](PF_6)$: $C_{52}H_{48}AgF_6N_{12}P$ (1093.24): calcd. C 57.10, H 4.42, N 15.37; found C 56. 87, H 4.32, N 15.47. IR (KBr): $\tilde{\nu}$ = 3435 (m, br.), 3145 (w), 2923 (w), 1584 (w), 1552 (m), 1497 (w), 1446 (s), 1396 (m), 1355 (m), 1265 (m), 966 (m), 841 (s), 752 (m), 698 (w), 558 (m) cm^{-1}. ^{1}H NMR (500 MHz, CD_3CN): δ = 1.78 (s, 6 H, $CH_3^{ar2,6}$), 2.33 (s, 3 H, CH_3^{pz3}), 2.40 (s, 3 H, CH_3^{ar4}), 6.51 (s, 1 H, CH^{pz4}), 7.00 (s, 2 H, $CH^{ar3,5}$), 7.17 (m, 3 H, CH^{ph}), 7.25 (m, 2 H, CH^{ph}) 7.35 (d, ^3J = 2.0 Hz, 1 H, CH^{im4}), 7.83 (d, ^3J = 9.5 Hz, 1 H, CH^{pdz}), 8.04 (d, ^3J = 2.0 Hz, 1 H, CH^{im5}), 8.13 (d, ^3J = 9.5 Hz, 1 H, CH^{pdz}) ppm. ^{13}C NMR (125 MHz, CD_3CN): δ = 14.1 (CH_3^{pz3}), 17.5 ($CH_3^{ar2,6}$), 21.3 (CH_3^{ar4}), 112.2 (C^{pz4}), 121.5 (C^{im5}), 124.6 (C^{pdz}), 125.7 (C^{im4}), 126.4 (C^{pdz}), 129.5 ($C^{ph2,6}$), 129.6 (C^{ph4}), 129.7 ($C^{ph3,5}$), 130.3 ($C^{ar3,5}$), 131.5 (C^{ph1}), 135.6 ($C^{ar2,6}$), 136.7 (C^{ar1}), 140.7 (C^{ar4}), 146.5 (C^{pz5}), 153.7 (C^{pz3}), 154.2 (C^{pdz}), 156.6 (C^{pdz}), 183.7 (C^{im2}) ppm. ^{1}H NMR (500 MHz, [D$_6$]acetone, 233 K): δ = 1.72 (s, 6 H, $CH_3^{ar2,6}$), 2.32 (s, 3 H, CH_3^{pz3}), 2.44 (s, 3 H, CH_3^{ar4}), 6.58 (s, 1 H, CH^{pz4}), 7.08 (s, 2 H, $CH^{ar3,5}$), 7.12 (m, 3 H, CH^{ph}), 7.42 (m, 2 H, CH^{ph}) 7.76 (d, ^3J = 2 Hz, 1 H, CH^{im4}), 8.18 (d, ^3J = 9.5 Hz, 1 H, CH^{pdz}), 8.51 (d, ^3J = 2 Hz, 1 H, CH^{im5}), 8.53 (d, ^3J = 8.7 Hz, 1 H, CH^{pdz}) ppm. MS (ESI^+): *m/z* (%) = 949.2 (100) $[L_2Ag]^+$. MS (ESI^-): *m/z* (%) = 144.9 (100) $[PF_6]^-$. HRMS (ESI^+): calcd. for $C_{52}H_{48}AgN_{12}$ 947.3170; found 947.3158.

Complex $[(L^3)_2Ag_2](PF_6)(BF_4)$ (6): Complex **6** was prepared by addition of 1 equiv. of $AgBF_4$ to a solution of $[(L^3)_2Ag](PF_6)$ (**4**) in acetone. Crystallization by slow diffusion of diethyl ether into an acetone solution at room temperature afforded colourless crystals of **6**. $C_{42}H_{44}Ag_2BF_{10}N_{12}P$ (1164.07): calcd. C 43.32, H 3.81, N 14.44; found C 43.93, H 3.54, N 14.15. ^{1}H NMR (500 MHz, [D$_6$]acetone, 233 K): δ = 2.13 (s, 3 H, CH_3^{pz3}), 2.16 (s, 6 H, $CH_3^{ar2,6}$), 2.33 (s, 3 H, CH_3^{ar4}), 2.70 (s, 3 H, CH_3^{pz5}), 6.53 (s, 1 H, CH^{pz4}), 7.15 (s, 2 H, $CH^{ar3,5}$), 7.99 (s, 1 H, CH^{im4}), 8.57 (s, 1 H, CH^{im5}), 8.75 (s, 2 H, CH^{pdz}) ppm. ^{13}C NMR (125 MHz, [D$_6$]acetone, 233 K): δ = 13.9 (CH_3^{pz3}), 14.2 (CH_3^{pz5}), 17.9 ($CH_3^{ar2,6}$), 20.8 (CH_3^{ar4}), 112.8 (C^{pz4}), 118.9, 123.3, 125.7, 126.5, 126.9, 135.5 ($C^{ph2,6}$), 136.2, 140.5, 145.5, 153.3, 154.3, 154.5, 181.3 (C^{im2}) ppm. (300 MHz, [D$_6$]acetone, 293 K): δ = 2.09 (s, 6 H, $CH_3^{ar2,6}$), 2.20 (s, 3 H, CH_3^{pz3}), 2.37 (s, 3 H, CH_3^{ar4}), 2.69 (s, 3 H, CH_3^{pz5}), 6.51 (s, 1 H, CH^{pz4}), 7.12 (s, 2 H, $CH^{ar3,5}$), 7.86 (d, ^3J = 1.9 Hz, 1 H, CH^{im4}), 8.41 (d, ^3J = 1.9 Hz, 1 H, CH^{im5}), 8.65 (d, ^3J = 9.5 Hz, 1 H, CH^{pdz}), 8.70 (d, ^3J = 9.5 Hz, 1 H, CH^{pdz}) ppm. ^{13}C NMR (75 MHz, [D$_6$]acetone, 293 K): δ = 14.0 (CH_3^{pz3}), 14.5 (CH_3^{pz5}), 18.0 ($CH_3^{ar2,6}$), 21.1 (CH_3^{ar4}), 113.1 (C^{pz4}), 123.1 (C^{im5}), 126.1 (C^{pdz}), 126.8 (C^{im4}), 129.3 (C^{pdz}), 130.2 ($C^{ar3,5}$), 135.7 ($C^{ar2,6}$), 136.8 (C^{ar1}), 140.8 (C^{ar4}), 145.7 (C^{pz5}), 154.1 (C^{pdz}), 154.9 (C^{pdz}), 155.1 (C^{pz3}), 189.4 (C^{im2}) ppm.

Complex $[(L^3)_2Ag_3](PF_6)(BF_4)_2$ (7): Complex **7** was prepared by addition of 2 equiv. of $AgBF_4$ to a solution of complex $[(L^3)_2Ag](PF_6)$ (**4**) in acetone. Crystallization by slow diffusion of diethyl ether into this acetone solution at room temperature afforded a few colourless crystals. Satisfactory elemental analysis could not be obtained because of the small amount of crystalline material. ^{1}H NMR (300 MHz, [D$_6$]acetone): δ = 2.11 (s, 6 H, $CH_3^{ar2,6}$), 2.15 (s, 3 H, CH_3^{pz3}), 2.36 (s, 3 H, CH_3^{ar4}), 2.70 (s, 3 H, CH_3^{pz5}), 6.49 (s, 1 H, CH^{pz4}), 7.12 (s, 2 H, $CH^{ar3,5}$), 7.86 (d, ^3J = 2.0 Hz, 1 H, CH^{im4}), 8.42 (d, ^3J = 2.0 Hz, 1 H, CH^{im5}), 8.64 (d, ^3J = 9.5 Hz, 1 H, CH^{pdz}), 8.68 (d, ^3J = 9.5 Hz, 1 H, CH^{pdz}) ppm. ^{13}C NMR (75 MHz, [D$_6$]-acetone): δ = 14.1 (CH_3^{pz3}), 14.4 (CH_3^{pz5}), 18.1 ($CH_3^{ar2,6}$), 21.0 (CH_3^{ar4}), 113.2 (C^{pz4}), 123.6 (C^{im5}), 126.3 (C^{pdz}), 126.9 (C^{im4}),

130.2 ($C^{ar3,5}$), 130.5 (C^{pdz}) 135.8 ($C^{ar2,6}$), 136.9 (C^{ar1}), 140.8 (C^{ar4}), 145.9 (C^{pz5}), 153.9 (C^{pdz}), 154.7 (C^{pdz}), 155.2 (C^{pz3}), 181.8 (C^{im2}) ppm.

Supporting Information (see footnote on the first page of this article): Figures of the molecular structures of $HL^1(BF_4)$, $HL^4(BF_4)$, and $HL^5(PF_6)$; details of the crystallographic data.

Acknowledgments

Support by the Fonds der Chemischen Industrie is gratefully acknowledged. We thank Dr. Holm Frauendorf and his team (Institute for Organic and Biomolecular Chemistry at the Georg August University) for collecting HRMS data.

[1] a) W. A. Herrmann, C. Köcher, *Angew. Chem. Int. Ed. Engl.* **1997**, *36*, 2163–2187; b) D. Bourissou, O. Guerret, F. P. Gabbai, G. Bertrand, *Chem. Rev.* **2000**, *100*, 39–91; c) W. A. Herrmann, *Angew. Chem. Int. Ed.* **2002**, *41*, 1290–1309; d) F. E. Hahn, M. C. Jahnke, *Angew. Chem. Int. Ed.* **2008**, *120*, 3166–3216; e) P. Frémonta, N. Marion, S. P. Nolan, *Coord. Chem. Rev.* **2009**, *253*, 862–892.

[2] a) S. P. Nolan, *N-Heterocyclic Carbenes in Synthesis*, Wiley-VCH, Weinheim, **2006**; b) F. Glorius, *N-Heterocyclic Carbenes in Transition Metal Catalysis*, Springer, Berlin, **2007**.

[3] a) E. Peris, R. H. Cabtree, *Coord. Chem. Rev.* **2004**, *248*, 2239–2246; b) O. Kühl, *Chem. Soc. Rev.* **2007**, *36*, 592–607; c) D. Pugh, A. A. Danopoulos, *Coord. Chem. Rev.* **2007**, *251*, 610–641; d) H. M. Lee, C.-C. Lee, P.-Y. Cheng, *Curr. Org. Chem.* **2007**, *11*, 1491–1524; e) M. Poyatos, J. A. Mata, E. Peris, *Chem. Rev.* **2009**, *109*, 3677–3707; f) A. John, P. Ghosh, *Dalton Trans.* **2010**, *39*, 7183–7206.

[4] a) Y. Zhou, W. Chen, *Organometallics* **2007**, *26*, 2742–2746; b) U. J. Scheele, M. John, S. Dechert, F. Meyer, *Eur. J. Inorg. Chem.* **2008**, *3*, 373–377; c) U. J. Scheele, M. Georgiou, M. John, S. Dechert, F. Meyer, *Organometallics* **2008**, *27*, 5146–5151; d) Y. Zhou, X. Zhang, W. Chen, H. Qiu, *J. Organomet. Chem.* **2008**, *693*, 205–215; e) S.-J. Jeon, R. M. Waymouth, *Dalton Trans.* **2008**, *4*, 437–439; f) M. Georgiou, S. Wöckel, V. Konstanzer, S. Dechert, M. John, F. Meyer, *Z. Naturforsch., Teil B* **2009**, *64*, 1542–1552.

[5] See, for example: a) F. E. Hahn, C. Radloff, T. Pape, A. Hepp, *Chem. Eur. J.* **2008**, *14*, 10900–10904; b) M. C. Jahnke, M. Hussain, F. Hupka, T. Pape, S. Ali, F. E. Hahn, K. J. Cavell, *Tetrahedron* **2009**, *65*, 909–913; c) J. Ye, S. Jin, W. Chen, H. Qiu, *Inorg. Chem. Commun.* **2008**, *11*, 404–408; d) Y.-H. Chang, Z.-Y. Liu, Y.-H. Liu, S.-M. Peng, J.-T. Chen, S.-T. Liu, *Dalton Trans.* **2011**, *40*, 489–494.

[6] See, for example: a) E. K. van den Beuken, B. Feringa, *Tetrahedron* **1998**, *54*, 12985–13011; b) B. Bosnich, *Inorg. Chem.* **1999**, *38*, 2554–2562; c) F. Meyer, *Eur. J. Inorg. Chem.* **2006**, 3789–3800; d) S. Matsunaga, M. Shibasaki, *Bull. Chem. Soc. Jpn.* **2008**, *81*, 60–75; e) M. Delferro, T. J. Marks, *Chem. Rev.* **2011**, DOI: doi.org/10.1021/cr1003634.

[7] a) A. L. Gavrilova, B. Bosnich, *Chem. Rev.* **2004**, *104*, 349–383; b) J. Klingele, S. Dechert, F. Meyer, *Coord. Chem. Rev.* **2009**, *253*, 2698–2741.

[8] a) D. E. Fenton, H. Okawa, *Chem. Ber./Recueil* **1997**, *130*, 433–442; b) M. Jarenmark, H. Carlsson, E. Nordlander, *C. R. Chim.* **2007**, *10*, 433–462; c) M. Andruh, *Chem. Commun.* **2011**, *47*, 3025–3042.

[9] N. Wheatley, P. Kalck, *Chem. Rev.* **1999**, *99*, 3379–3419.

[10] a) S. Brooker, *Eur. J. Inorg. Chem.* **2002**, *10*, 2535–2547; b) U. Beckmann, S. Brooker, *Coord. Chem. Rev.* **2003**, *245*, 17–29.

[11] a) Z. Xu, L. K. Thompson, in *Comprehensive Coordination Chemistry II* (Eds.: J. A. McCleverty, T. J. Meyer), Elsevier Ltd., Oxford, **2004**, vol. 1, p. 63–95; b) U. J. Scheele, S. Dechert, F. Meyer, *Tetrahedron Lett.* **2007**, *48*, 8366–8370.

[12] U. J. Scheele, S. Dechert, F. Meyer, *Chem. Eur. J.* **2008**, *14*, 5112–5115.

[13] a) K.-M. Lee, J. C. C. Chen, I. J. B. Lin, *J. Organomet. Chem.* **2001**, *617*, 364–375; b) U. J. Scheele, S. Dechert, F. Meyer, *Inorg. Chim. Acta* **2006**, *359*, 4891–4900; c) B. Liu, W. Chen, S. Jin, *Organometallics* **2007**, *26*, 3660–3667; d) J. Ye, X. Zhang, W. Chen, S. Shimada, *Organometallics* **2008**, *27*, 4166–4172.

[14] a) P. L. Arnold, *Heteroat. Chem.* **2002**, *13*, 534–539; b) J. C. Garrison, W. J. Youngs, *Chem. Rev.* **2005**, *105*, 3978–4008; c) J. C. Y. Lin, R. T. W. Huang, C. S. Lee, A. Bhattacharyya, W. S. Hwang, I. J. B. Lin, *Chem. Rev.* **2009**, *109*, 3561–3598.

[15] a) M. A. Omary, M. A. Rawashdeh-Omary, H. V. K. Diyabalanage, H. V. R. Dias, *Inorg. Chem.* **2003**, *42*, 8612–8614; b) Y. Zhou, X. Zhang, W. Chen, H. Qiu, *J. Organomet. Chem.* **2008**, *693*, 205–215.

[16] I. J. B. Lin, C. S. Vasam, *Coord. Chem. Rev.* **2007**, *251*, 642–670.

[17] O. Guerret, S. Solé, H. Gornitzka, M. Teichert, G. Trinquier, G. Bertrand, *J. Am. Chem. Soc.* **1997**, *119*, 6668–6669.

[18] A. A. D. Tulloch, A. A. Danopoulos, S. Winston, S. Kleinhenz, G. Eastham, *J. Chem. Soc., Dalton Trans.* **2000**, *24*, 4499–4506.

[19] H. M. J. Wang, I. J. B. Lin, *Organometallics* **1998**, *17*, 972–975.

[20] Q. Yu, A.-S. Zhang, T.-L. Hu, X.-H. Bu, *Solid State Sci.* **2010**, *12*, 1484–1489.

[21] U. J. Scheele, Dissertation, Universität Göttingen, **2008**.

[22] L. K. Thompson, T. C. Woon, D. B. Murphy, E. J. Gabe, F. L. Lee, Y. Le Page, *Inorg. Chem.* **1985**, *24*, 4719–4725.

[23] G. Steiner, J. Gries, D. Lenke, *J. Med. Chem.* **1981**, *24*, 59–63.

[24] T. Steiner, *Acta Crystallogr., Sect. B* **1998**, *54*, 456–463.

[25] No further changes are detected upon addition of even more $AgBF_4$.

[26] M. Jansen, *Angew. Chem. Int. Ed. Engl.* **1987**, *26*, 1098–1110.

[27] A. Bondi, *J. Phys. Chem.* **1964**, *68*, 441–451.

Received: March 16, 2011
Published Online: July 4, 2011

